



OPEN

SUBJECT AREAS:
CANCER PREVENTION
CELL INVASIONReceived
5 August 2014Accepted
21 October 2014Published
11 November 2014Correspondence and
requests for materials
should be addressed to
J.Y.M. (jyma@kiom.re.
kr)

Reduction of metastatic and angiogenic potency of malignant cancer by *Eupatorium fortunei* via suppression of MMP-9 activity and VEGF production

Aeyung Kim, Minju Im, Nam-Hui Yim & Jin Yeul Ma

Korean Medicine (KM)-Based Herbal Drug Development Group, Korea Institute of Oriental Medicine (KIOM), 483 Expo-ro, Yuseong-gu, Daejeon 305-811, Republic of Korea.

Eupatorium fortunei has long been used to treat nausea and poor appetite, and has been prescribed as a diuretic and detoxifying drug in Chinese medicine. Recent studies have demonstrated that *E. fortunei* possesses anti-bacterial, anti-oxidant, and anti-diabetic activities, as well as cytotoxicity to human leukemia cells. However, at non-toxic concentrations, the effects of an aqueous extract of *E. fortunei* (WEF) on the metastatic and angiogenic potential of malignant tumor cells have not been reported. In this study, we found that WEF suppressed the metastatic properties, including anchorage-independent colony formation, migration, and invasion, by downregulating the proteolytic activity of MMP-9. NF- κ B activation and the phosphorylation of p38 and JNK were reduced significantly by WEF. Additionally, WEF inhibited tumor-induced angiogenesis markedly, affecting HUVEC migration, tube formation by HUVECs, and microvessel sprouting from rat aortic rings via a reduction in VEGF in tumors. In a pulmonary metastasis model, daily administration of WEF at 50 mg/kg markedly decreased metastatic colonies of intravenously injected B16F10 cells on the lung surface in C57BL/6J mice. Further, none of the WEF-administered mice exhibited systemic toxicity. Taken together, our results indicate that WEF is a potential therapeutic herbal product that may be useful for controlling malignant metastatic cancer.

The aggressive growth and metastatic spread of tumor cells is a hallmark of malignant tumors and results in high mortality among cancer patients¹. Metastasis involves multiple processes, including a loss of adhesion between cells and the extracellular matrix (ECM), proteolytic degradation of the ECM, extravasation leading to invasion into new tissues, and colonization². Matrix metalloproteinases (MMPs) secreted by tumor cells, stromal fibroblasts, or infiltrating inflammatory cells, have been strongly implicated in multiple stages of the invasive and metastatic progression of tumor cells. Furthermore, MMPs participate in degradation of the vascular basement membrane and remodeling of the ECM during angiogenesis^{3–5}. In particular, MMP-9 is important for tumor angiogenesis by enhancing the availability of vascular endothelial cell growth factor (VEGF) in malignant tumors^{6–8}.

Angiogenesis, the formation of new blood vessels within a primary solid tumor or metastatic foci, plays a key role in supplying oxygen and nutrients for tumor growth, and it provides a path for cancer cell migration and filtration^{9,10}. Angiogenesis occurs by a complex step-wise process that includes proteolytic degradation of the basement membrane, the proliferation and migration/invasion of endothelial cells, and the formation of functional capillary lumens¹¹. One of the initial steps in tumor-induced angiogenesis is the secretion of multiple angiogenic factors from tumor cells, including VEGF, basic fibroblast growth factor (bFGF), and platelet-derived growth factor (PDGF). Among these, VEGF is the most important pro-angiogenic factor, and the level of VEGF is an important prognostic marker of tumor angiogenesis¹². The interaction of VEGF with its cognate receptor VEGFR on the surface of endothelial cells promotes the recruitment and proliferation of endothelial cells via the activation of PI3K/Akt and Ras/Raf/MEK/ERK signaling^{13,14}. Thus, the search for non-toxic agents that inhibit metastasis and tumor-induced angiogenesis via suppression of MMP-9 activity and VEGF secretion in tumor cells is a promising strategy for cancer therapy and prevention^{15–17}.

Eupatorium fortunei, known in Chinese as “Pei Lan,” has long been used as a diuretic and detoxifying drug in Chinese medicine and for the management of chill, dropsy, and fever. In a study aimed at identifying plants



antagonistic to soil-borne pathogens, a root extract of *E. fortunei* exerted a strong inhibitory effect against four microorganisms: *Streptomyces scabies* (potato scab), *Phytophthora megasperma* (root rot), *Verticillium dahliae* (wilt), and *Rhizoctonia solani* (damping off)¹⁸. Chen *et al.* reported that an aqueous extract of *E. fortunei* possessed significant anti-oxidant, anti-glycation, and anti-diabetic potential¹⁹. Additionally, *p*-cymene and neryl acetate, major components of *E. fortunei*, have been reported to possess anti-influenza activity. In a recent study, it was demonstrated that the ethyl acetate fraction of a methanol extract of *E. fortunei* exhibited cytotoxicity against human leukemia (HL-60) cells²⁰.

In the present study, we examined the inhibitory effect of an aqueous extract of *E. fortunei* (WEF) on the metastatic and angiogenic properties of malignant tumor cells *in vitro* and *in vivo*. Furthermore, we examined the detailed underlying mechanism of the anti-metastatic and -angiogenic activity of WEF, and investigated whether WEF intake suppressed the pulmonary metastasis of B16F10 melanoma cells after intravenous injection.

Results

WEF suppressed anchorage-independent B16F10 cell growth at non-cytotoxic doses. Prior to evaluating the *in vitro* anti-metastatic efficacy of WEF, we assessed the non-cytotoxic concentrations of WEF in B16F10 cells using MTT assays. As shown in Figure 1A, cell viability after treatment with WEF at concentrations ranging from 10 to 500 $\mu\text{g/ml}$ for 48 h was not significantly changed compared with untreated control cells; thus, we used WEF at concentrations of 25, 50, and 100 $\mu\text{g/ml}$ in all subsequent experiments. Metastatic malignant cells possess resistance to detachment-induced cell death, or “anoikis resistance,” which ensures anchorage-independent growth and survival during their dissemination²¹. As reported previously, B16F10 cells proliferate rapidly and form sizable colonies from a single cell in semi-solid agar²², whereas WEF treatment during incubation decreased the number of sizable colonies significantly and reduced colony size in a dose-dependent manner compared with untreated control B16F10 cells (Figure 1B). These results indicate that WEF suppressed metastatic colony formation by B16F10 cells with no apparent cytotoxicity at the concentrations used.

WEF suppressed B16F10 cell migration and invasion *in vitro*. To determine the influence of WEF on *in vitro* migration, we

investigated the wound healing activity of B16F10 cells in the presence or absence of WEF. As shown in Figure 2A, control B16F10 cells repaired the wounded area rapidly, leading to ~50% and ~80% healing at 18 h and 36 h, respectively. Meanwhile, WEF treatment inhibited wound repair significantly, in a dose-dependent manner, by ~50–90% and ~40–75% at 18 h and 36 h, respectively, compared with control cells. In a Transwell migration and invasion assay, WEF treatment reduced serum-induced migration and invasion markedly, to ~35–80% and ~10–45% of that in control cells, respectively (Figure 2B).

WEF intake inhibited the *in vivo* pulmonary metastasis of B16F10 cells with no adverse effects. Prior to examining the anti-metastatic effect of WEF *in vivo*, we checked whether repeated administration of WEF at 50 mg/kg induced systemic toxicity. Over 15 days, corresponding to the *in vivo* experiment period, WEF administration did not cause adverse effects such as a loss of body weight (Supplementary Table S1). The organ weights of control and WEF-treated mice were also similar (Supplementary Table S2). The aspartate aminotransferase/alanine aminotransferase and blood urea nitrogen/creatinine levels were not changed significantly by WEF administration, indicating that WEF did not aggravate hepatic or renal functions, respectively (Supplementary Table S3). Additionally, in hematological analyses, the RBC number, hemoglobin (Hb) level, leukocyte number, and other parameters were not significantly affected by WEF administration (Supplementary Table S4). Subsequent to this confirmation of safety, we assessed whether WEF intake suppressed pulmonary colonization by B16F10 cells after intravenous injection via the tail vein in C57BL/6J mice. In control mice, B16F10 cells metastasized to the lungs and formed numerous black colonies (1294 ± 213), while in WEF-administered mice the number of black colonies decreased significantly (550 ± 256) to ~40% of the level in control mice (Figure 3). These data indicate that WEF intake effectively suppressed the pulmonary metastasis of intravenously injected B16F10 cells with no apparent side effects.

WEF suppressed the metastatic potential of and inhibited phorbol myristate acetate (PMA)-induced MMP-9 expression and proteolytic activity in HT1080 cells. To clarify the anti-metastatic mechanism of WEF, well characterized conditions including HT1080 cells and PMA stimulation were used, as in previous studies^{22–26}. Similar to data obtained from B16F10 cells, WEF treatment significantly diminished the metastatic potential of HT1080 cells, including

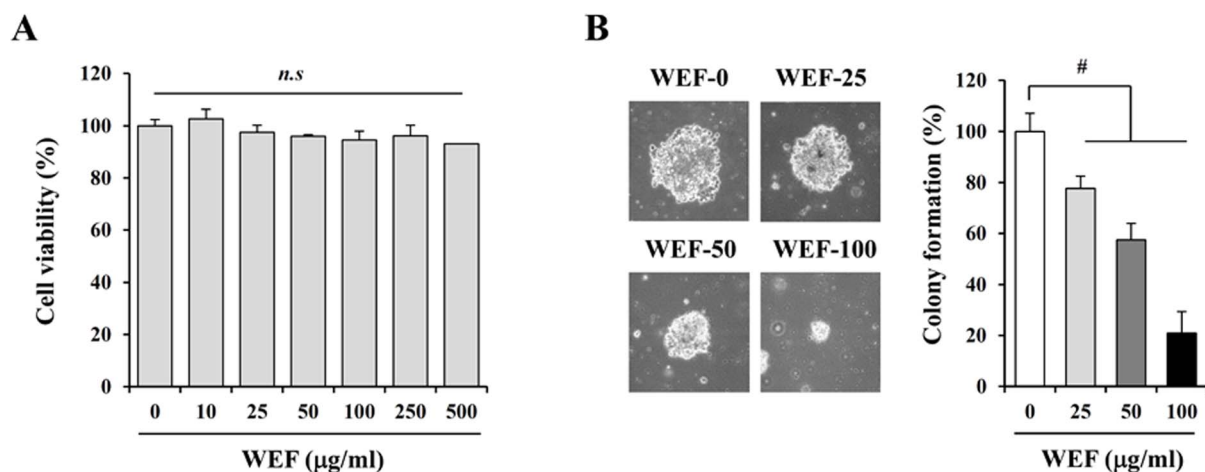


Figure 1 | WEF inhibits anchorage-independent growth of B16F10 cells. (A): Proliferation of cells (5×10^3 cells/well) incubated with 10 to 500 $\mu\text{g/ml}$ WEF for 48 h was measured by MTT assays. Data are the relative cell viability compared to untreated control and expressed as the mean \pm SD. *n.s.*, non-significant (B): Colony formation of B16F10 cells in soft agar in the presence of non-toxic concentrations of WEF (25, 50, and 100 $\mu\text{g/ml}$) was measured during 14-day-incubation. The diameters of 10 representative colonies were measured and expressed as the mean \pm SD. Data are representative of two independent experiments. #, $p < 0.01$ vs. untreated control.

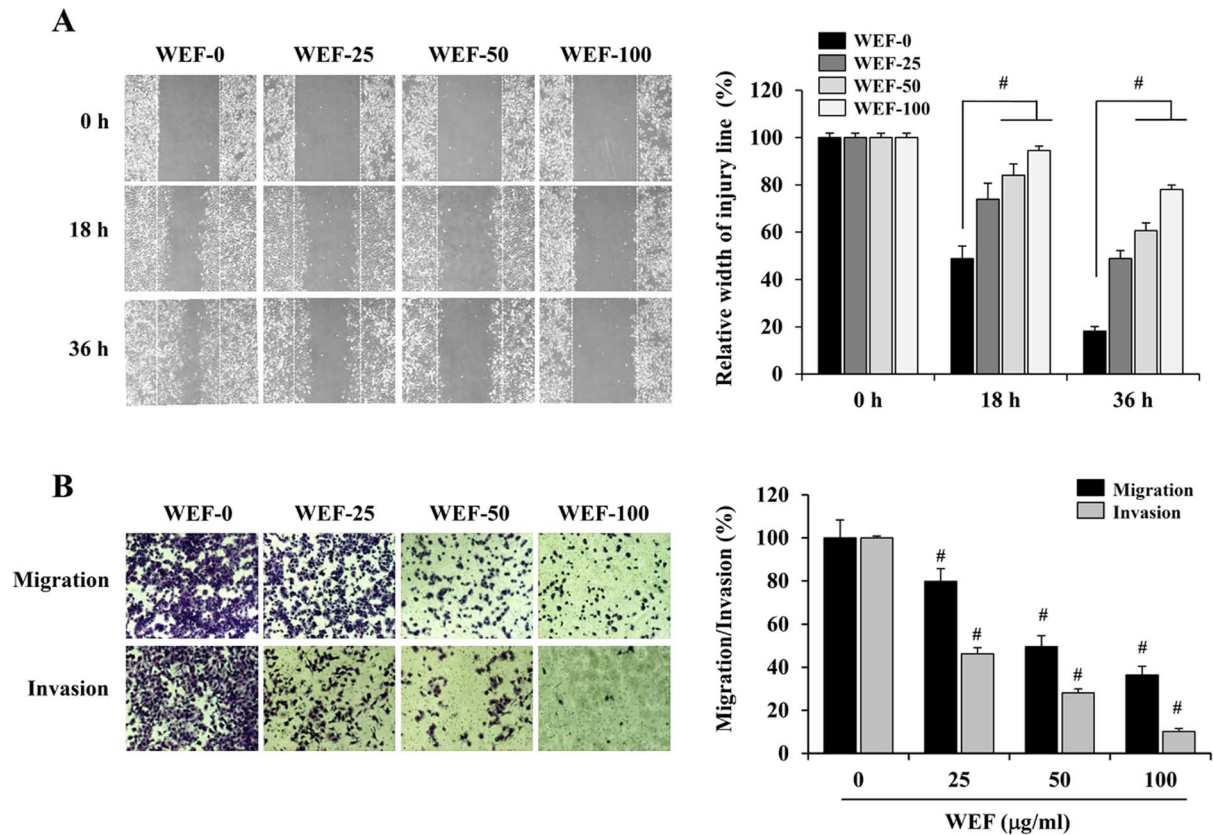


Figure 2 | WEF suppresses migration and invasion of B16F10 cells. (A): Cells grown to 90% confluence were treated with mitomycin C for 30 min and then wounded by scraping. Cells were incubated in the presence of 25, 50, and 100 μg/ml WEF and migration was monitored using phase-contrast microscopy after 18 and 36 h. Based on the width of wound at 0 h, relative width at 18 and 36 h was calculated and expressed as the mean ± SD of four selected fields. **(B):** Cells pre-treated with 25, 50, and 100 μg/ml WEF for 12 h were subjected to migrate and invade through Transwell for 24 h and 36 h, respectively. Cells migrated and invaded to the lower surface of the Transwell membrane were stained and relative migration and invasion were quantified using ImageJ software. Data are representative of three independent experiments and expressed as the mean ± SD of five random fields of each well. #, $p < 0.01$ vs. untreated control.

wound healing, migration, and invasion (Figure S1). It is known that MMP-2 and -9 are essential for the invasive capacity of malignant cancers by degrading the surrounding ECM and accelerating cancer metastasis and angiogenesis^{7,8,24}. We first examined the effects of WEF treatment on the transcriptional levels of various MMPs using RT-PCR. Control HT1080 cells expressed a considerable

amount of MMPs, including MMP-1, -2, -3, -9, -13, and -14, and uPA; in addition, PMA stimulation increased the levels of MMP-1, -3, -9, -13, and -14, and uPA. However, in cells pretreated with WEF, the PMA-induced increase in MMP-9 mRNA expression was almost completely blocked in a dose-dependent manner (Figure 4A), and the levels of MMP-14 and uPA were decreased slightly, compared

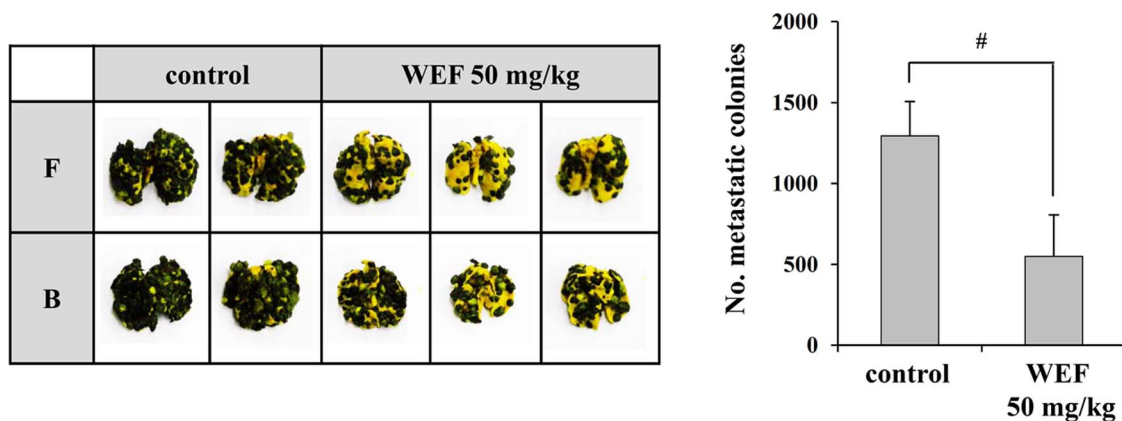


Figure 3 | Oral administration of WEF inhibits pulmonary metastasis of B16F10 cells. Five-week-old female C57BL/6J mice were intravenously injected via tail vein with B16F10 cells (3×10^5). After daily oral administration with saline (control) or WEF (50 mg/kg) for 17 days, mice were sacrificed and black colonies settled on the lung surface counted macroscopically after fixation. Images show metastatic colonies on the front (F) and back (B) side of the lungs. Metastatic colonies were counted and represented as the mean ± SD of each group (each group, $n = 4$). #, $p < 0.05$ vs. control.

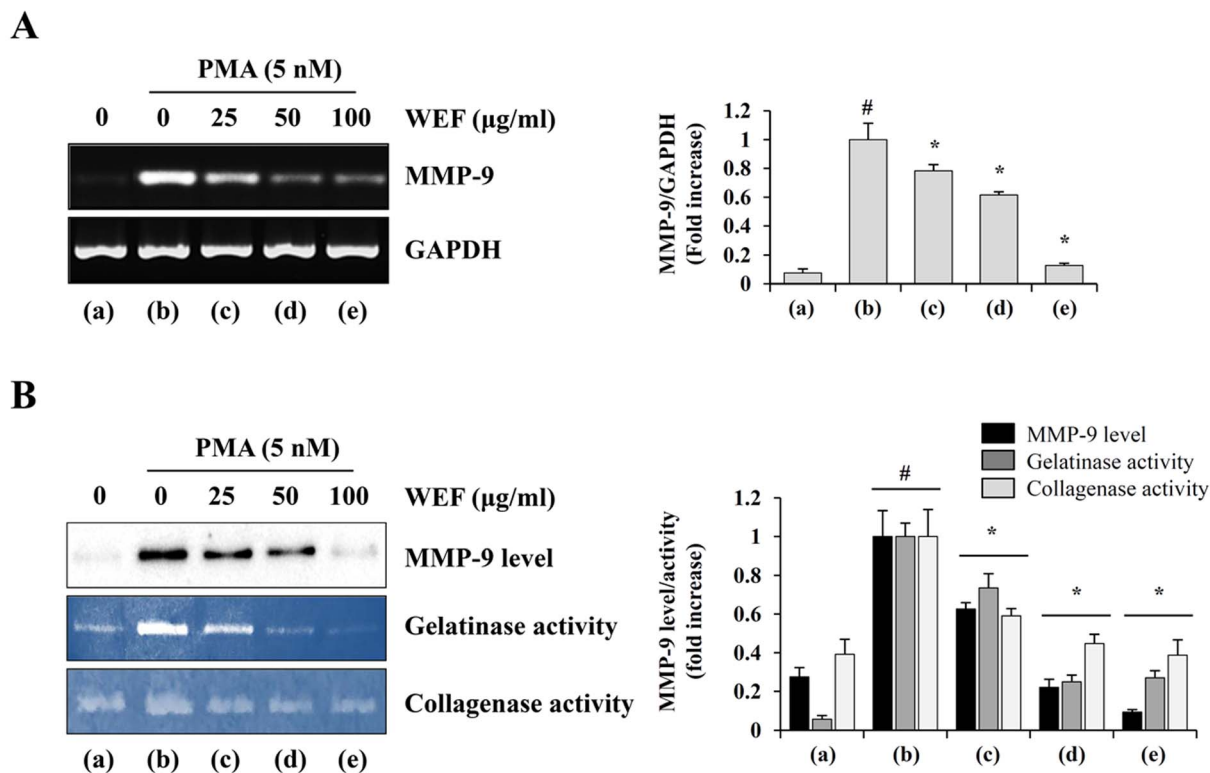


Figure 4 | WEF reduces PMA-induced MMP-9 expression and MMP-9 activity. HT1080 cells pretreated with 25, 50, and 100 $\mu\text{g/ml}$ WEF for 12 h in serum-free media were stimulated with 5 nM PMA for additional 24 h. (A): MMP-9 mRNA levels were measured by RT-PCR and relative expression was quantified after normalization to GAPDH. (B): CM were collected and analyzed for the MMP-9 level and MMP-9 activity by Western blotting and zymography, respectively. Gelatin and type I collagen were used as MMP-9 substrates. Data are expressed as the mean \pm SD of two independent experiments. The full size blot was shown in the Supplementary Figure S3 and band of interest is indicated with an arrow. #, $p < 0.01$ vs. untreated control. *, $p < 0.01$ vs. PMA stimulation.

with untreated control cells (Figure S2). Additionally, increases in MMP-9 secretion into the culture supernatant and the proteolytic activity of MMP-9 toward gelatin and type I collagen in response to PMA stimulation were reduced markedly by WEF treatment in a dose-dependent manner (Figure 4B). These results suggest that the downregulation of MMP-9 expression and its proteolytic activity by WEF attenuated the metastatic potential of HT1080 cells.

WEF suppressed PMA-induced p38 and JNK phosphorylation, and NF- κB activation. In previous reports, the activation of mitogen-activated protein kinases (MAPKs), including p38, ERK1/2, and JNK1/2, has been suggested to be important for the increase in MMP-9 expression and activity^{26,27}. As shown in Figure 5A, p38, ERK1/2, and JNK1/2 phosphorylation increased rapidly in control HT1080 cells in response to PMA stimulation. However, in WEF-treated cells, PMA-induced p38 and JNK phosphorylation was almost completely blocked. Because MAPKs act as upstream modulators of the transcription factor NF- κB , which is involved in MMP expression and invasion in various cancer cells²⁸, we next examined the effects of WEF on PMA-induced NF- κB activation. As shown in Figure 5A, I $\kappa\text{B}\alpha$ phosphorylation in control HT1080 cells was increased markedly by PMA stimulation and was accompanied by I $\kappa\text{B}\alpha$ degradation. However, in WEF-treated cells, PMA-induced I $\kappa\text{B}\alpha$ phosphorylation and degradation were almost completely inhibited, such that the increase in the p-I $\kappa\text{B}\alpha$ /I $\kappa\text{B}\alpha$ ratio was significantly lower in WEF-treated HT1080 cells than in control cells. Because NF- κB activation also requires nuclear translocation of the p65 subunit of NF- κB , we examined the cytoplasmic and nuclear pool of p65 by Western blotting. As shown in Figure 5B, in control cells the p65 subunit translocated from the cytosol to the nucleus

with PMA stimulation, whereas WEF treatment effectively blocked p65 nuclear translocation in a dose-dependent manner. Collectively, these results indicate that WEF suppressed the metastatic potential of HT1080 cells by reducing MMP-9 activity via inhibition of p38, JNK, and NF- κB activation. In B16F10 cells, TNF- α was used as an inducer of MMP-9 and NF- κB activation^{29,30}. As demonstrated in HT1080 cells, TNF- α -induced increases in the MMP-9 mRNA expression and MMP-9 gelatinolytic activity were significantly decreased by WEF treatment. In addition, WEF treatment effectively prevented the increase in the ratio of p-I $\kappa\text{B}\alpha$ /I $\kappa\text{B}\alpha$ and slightly inhibited phosphorylation of p38 and JNK in response to TNF- α stimulation (Figure S5).

WEF suppressed tumor-induced angiogenesis *in vitro* and *in vivo*. Tumor-induced angiogenesis, new blood vessel formation within solid tumors, is essential for growth, invasion, and metastasis, and depends on the secretion of angiogenic factors such as VEGF and bFGF by tumor cells and macrophages into the ECM^{14,31}. It has been demonstrated that supernatants from various tumor cells, including HT1080, A549, SW620, NCI-H460, and CL1-5 cells, trigger angiogenic responses³²⁻³⁴. To examine the effects of WEF on tumor-induced angiogenesis, we first evaluated the ability of HUVECs to form tube-like structures on Matrigel after incubation with WEF-treated or -untreated conditioned media (CM) from HT1080 or PC-3 cells. As shown in Figure 6A, CM from control HT1080 and PC-3 cells induced robust tube formation. However, compared with CM from control cells, the WEF-treated CM did not cause a significant increase in the tube network, resulting in a reduced number, length, and area of capillary-like structures, in a dose-dependent manner. During tumor-induced angiogenesis, cancer cells strongly attract endothelial cells by secreting pro-angiogenic factors. To evaluate the

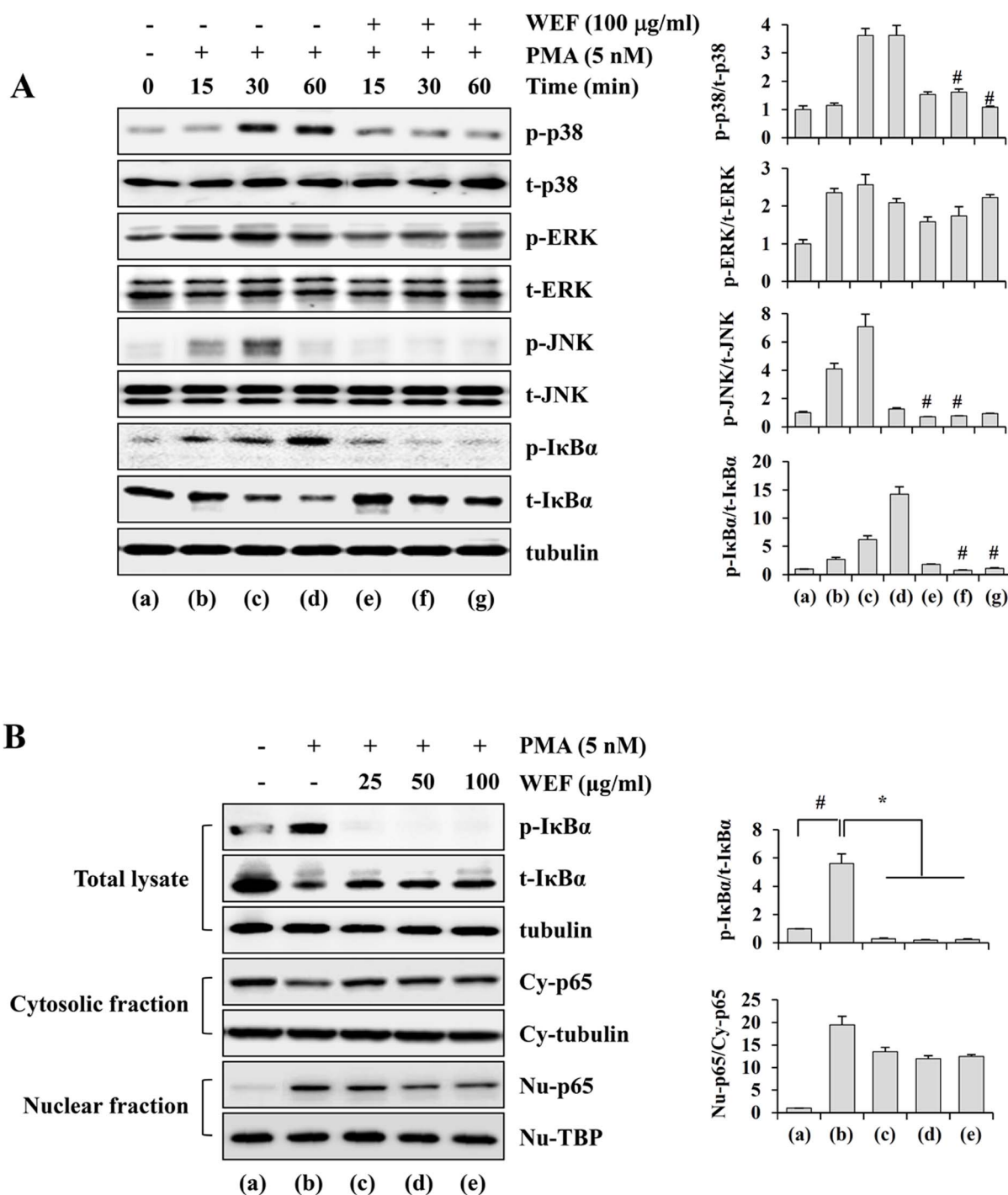


Figure 5 | WEF suppresses PMA-induced p38 and JNK phosphorylation as well as NF- κ B activation. (A): After treatment with or without WEF (100 $\mu\text{g/ml}$) for 12 h, cells were stimulated with PMA (5 nM) for 15, 30, or 60 min. Total cell lysates were subjected to Western blotting to evaluate phosphorylation of p38, ERK, and JNK. Phosphorylation and degradation of I κ B α were also measured. After normalization to tubulin, the relative ratios of phosphorylated protein/total protein were calculated. (B): Cells pre-treated with WEF (25, 50, or 100 $\mu\text{g/ml}$) for 12 h were stimulated with PMA for 30 min and then subjected to Western blotting. Total cell lysates were measured for I κ B α phosphorylation and degradation. Cytosolic and nuclear fractions were prepared to evaluate nuclear translocation of the NF- κ B p65 subunit after PMA stimulation. Tubulin and TBP were used as loading control for cytosolic and nuclear compartment, respectively. Data are expressed as the mean \pm SD of two independent experiments. The full size blots were shown in the Supplementary Figure S4 and band of interest is indicated with an arrow. #, $p < 0.01$ vs. untreated control. *, $p < 0.01$ vs. PMA stimulation.

effects of WEF on tumor-induced endothelial cell migration, HUVECs and WEF-treated PC-3 cells were seeded in the upper and lower chambers of Transwells, respectively, and then HUVECs were allowed to migrate for 24 h. As shown in Figure 6B, control PC-3 cells in the lower chamber strongly induced HUVEC migration. WEF treatment prevented PC-3 cells from attracting HUVECs in a dose-

dependent manner, indicating that WEF suppressed the tumor cell-derived chemotactic motility of endothelial cells. To confirm the anti-angiogenic effects of WEF-treated PC-3 cells *in vivo*, a Matrigel plug assay was performed in athymic nude mice. As reported earlier³⁵, PC-3 cells trapped in growth factor-reduced Matrigel increased angiogenesis in the plugs markedly, exhibiting a bright red color (Figure 6C). In the

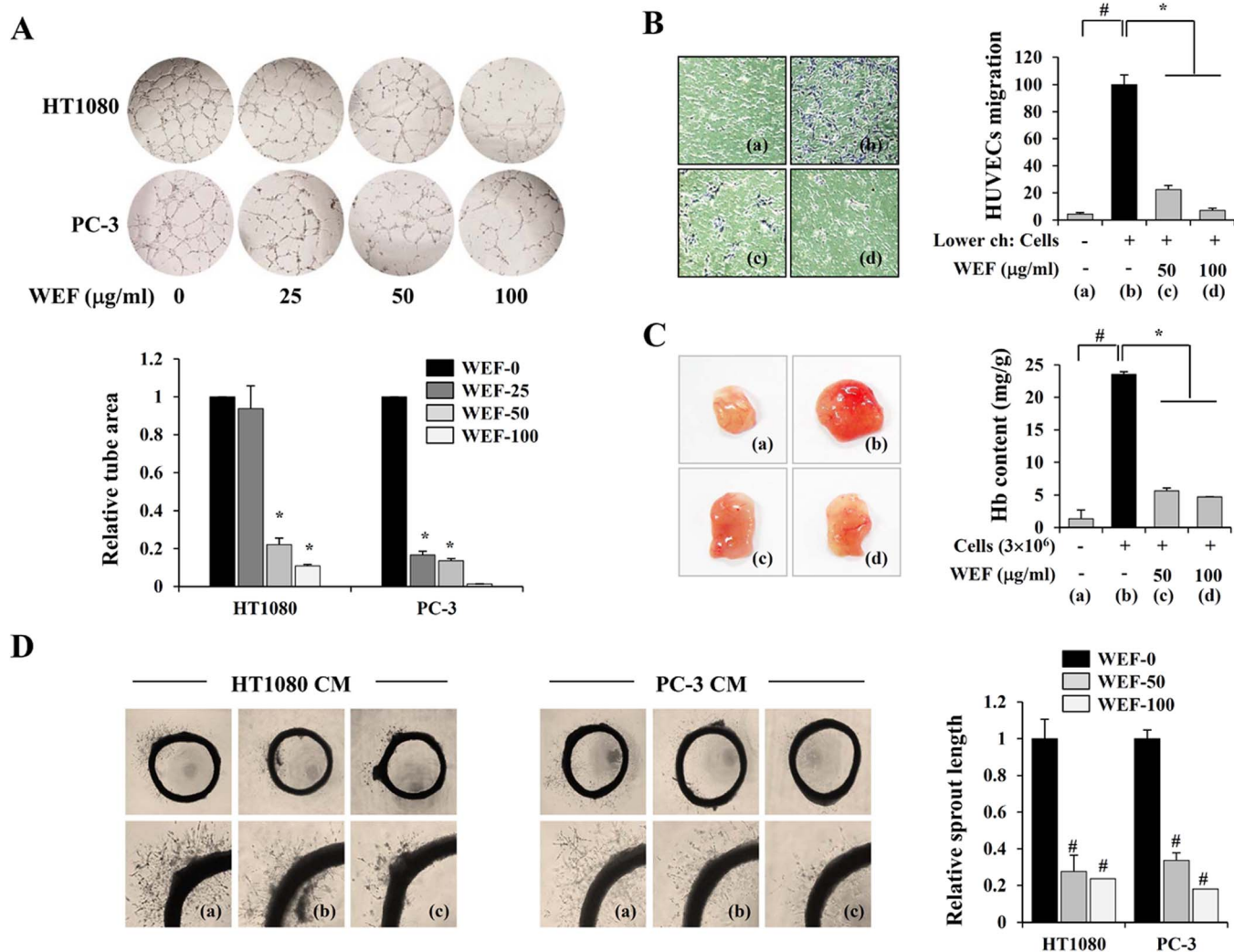


Figure 6 | WEF suppresses tumor-induced angiogenesis. (A): Capillary-like tube formation by HUVECs induced by control CM or WEF-treated CM of HT1080 or PC-3 cells was examined. The total tube area was measured using ImageJ software and expressed as the mean \pm SD of three random fields. #, $p < 0.01$ vs. untreated control. (B): PC-3 cells treated or untreated with WEF for 12 h were plated in the lower chamber of Transwell and incubated in 0.5% serum media. HUVECs suspended in 0.5% serum media were added to the upper chamber and allowed to migrate across Transwell. After 24 h, HUVECs migrated to the lower surface were stained and quantified using ImageJ software. #, $p < 0.01$ vs. no PC-3 cells. *, $p < 0.01$ vs. WEF-untreated PC-3 cells. (C): PC-3 cells ($3 \times 10^6/100 \mu\text{l}$) suspended in serum-free RPMI were mixed with Matrigel, heparin, and WEF (0, 50, and 100 $\mu\text{g/ml}$). Matrigel mixture was subcutaneously implanted into the ventral region of athymic nude mice. On day 14, Matrigel plugs were carefully removed and Hb contents in plugs were quantified using Drabkin's reagent kit. Data represent the mean \pm SD ($n=3$). #, $p < 0.01$ vs. Matrigel alone. *, $p < 0.01$ vs. WEF-untreated PC-3 cells. (D): Freshly prepared aortic rings were placed in a Matrigel-coated 48-well culture plate, incubated in EGM-2 for 3 days, and then replaced with control CM or WEF-treated CM of HT1080 or PC-3 cells. After 3 days, sprouts from rat aortic rings were photographed and sprout length was quantified. Data are expressed as the mean \pm SD ($n=3$) #, $p < 0.01$ vs. untreated control.

presence of WEF, angiogenesis was inhibited and Hb levels were decreased significantly, by 75–80%, in a dose-dependent manner. Tumor growth was also suppressed by WEF, with a 30–40% plug weight reduction, suggesting that WEF inhibited angiogenesis initially and then suppressed tumor growth. Next, the effects of WEF-treated CM on microvessel sprout formation were determined using a rat aortic ring assay, a widely used *ex vivo* angiogenesis assay in which several stages of angiogenesis, including endothelial cell proliferation, migration, and tube formation, occur^{36,37}. As shown in Figure 6D, WEF-untreated control CM from HT1080 and PC-3 cells effectively triggered microvessel sprouting around the aortic rings. However, the sprout length around aortic rings incubated with WEF-treated CM was relatively shorter than that around control CM, suggesting that WEF antagonized tumor-induced angiogenesis. To test whether the inhibitory effect of WEF-treated CM was reversible, the CM was removed and the rings were further

incubated with EGM-2 media for an additional 3 days. Replacement with EGM-2 media resulted in renewed vessel sprout formation (Figure S6), indicating that the inhibition of vessel sprout formation by WEF-treated CM was reversible and not due to cytotoxicity.

WEF decreased VEGF- α production by suppressing HIF-1 α accumulation and the Akt/mTOR pathway. The induction of new blood vessel formation by tumor cells, tumor angiogenesis, is closely associated with VEGF- α production. As shown in Figure 7A, the mRNA levels of VEGF- α in HT1080 and PC-3 cells were high, but WEF treatment decreased VEGF- α mRNA expression in a dose-dependent manner. The protein level of VEGF- α in the CM was also suppressed by WEF treatment (Figure 7B). Because VEGF- α is an immediate downstream target of HIF-1 α ³⁸, we examined whether WEF inhibited HIF-1 α protein accumulation and Akt/mTOR signal transduction under CoCl_2 treatment conditions, mimicking

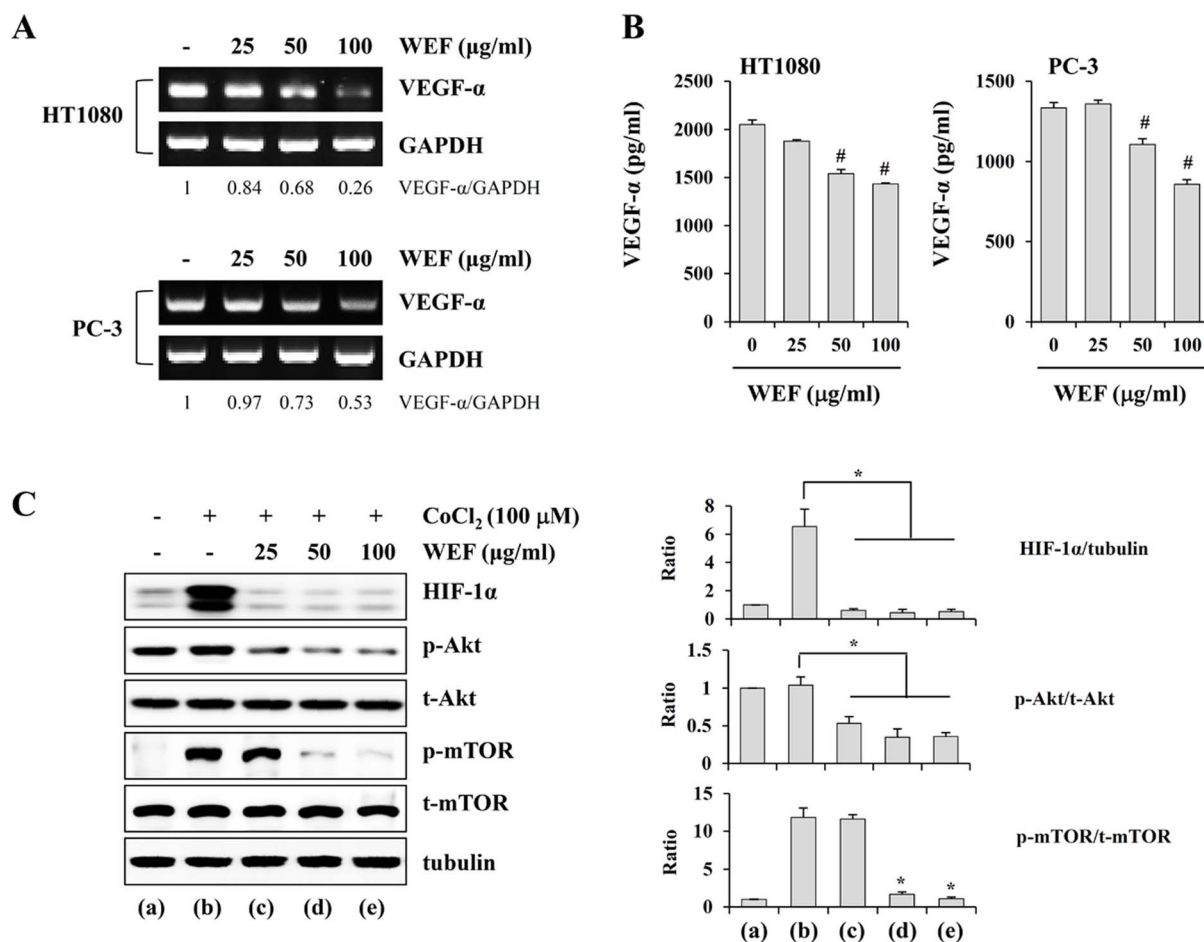


Figure 7 | WEF inhibits VEGF- α production and HIF-1 α expression. (A): HT1080 and PC-3 cells were treated with 25, 50, and 100 μ g/ml WEF for 24 h and VEGF- α mRNA levels were measured by RT-PCR. Relative ratio was quantified after normalization to GAPDH. (B): HT1080 and PC-3 cells were treated with WEF (25, 50, and 100 μ g/ml) for 48 h, and the level of VEGF- α in CM was determined by ELISA. #, $p < 0.01$ vs. untreated control. (C): PC-3 cells were pretreated with WEF (25, 50, and 100 μ g/ml) for 12 h, and then stimulated with 100 μ M CoCl₂ for 6 h. Total cell lysates were subjected to Western blotting to measure the levels of HIF-1 α , phosphorylated Akt and mTOR. After normalization to tubulin, the relative ratios were calculated. Data are expressed as the mean \pm SD of two independent experiments. The full size blots were shown in the Supplementary Figure S10 and band of interest is indicated with an arrow. #, $p < 0.01$ vs. untreated control.

physiological hypoxia. WEF decreased CoCl₂-stimulated Akt and mTOR phosphorylation markedly, consistent with their inhibitory effects on HIF-1 α protein accumulation (Figure 7C and Figure S7). In B16F10 cells, WEF treatment decreased VEGF- α mRNA expression dose-dependently, and remarkably suppressed CoCl₂-stimulated HIF-1 α protein accumulation and Akt and mTOR phosphorylation (Figure S8). However, WEF did not affect bFGF- and VEGF- α -induced angiogenesis in Matrigel plugs; indeed, bFGF and VEGF- α induced tube formation in HUVECs, and EGM-2 induced the migration of HUVECs (Figure S9), suggesting that WEF exerted its anti-angiogenic influence by targeting cancer cells but not endothelial cells.

Discussion

Solid tumors require angiogenesis, the formation of new blood vessels from pre-existing ones, for growth and metastasis. Without angiogenesis, tumor growth is restricted to a few millimeters and tumor cells cannot escape into the circulation to metastasize⁹. *In vivo*, tumor-induced angiogenesis begins when tumor cells make an 'angiogenic switch' by releasing pro-angiogenic factors such as VEGF, bFGF, angiopoietin, and MMPs, which, in turn, stimulate existing blood vessels to initiate angiogenesis¹⁷. In a study by Zheng *et al.*, MMP-2, MMP-9, and VEGF expression was found to

be associated positively with tumor size, invasive depth, lymphatic and venous invasion, and lymph node metastasis and to be intimately involved in the growth, angiogenesis, and progression of gastric carcinomas⁷. Recent studies have reported that invasive cells express MMP-9 at higher levels and that its expression is closely linked with vascular invasion and aggressive malignant phenotypes. Increased VEGF expression is closely associated with increased intratumoral microvessel density and a poor prognosis in breast cancer patients^{7,39}. Thus, the discovery of agents to inhibit the production of pro-angiogenic factors in tumor cells is a promising strategy that can limit the spread of cancer cells to a new site, improving the efficacy of cancer therapy and cancer patient survival.

E. fortunei has been used medicinally in both Japan and China. In traditional Chinese medicine, it has been prescribed for nausea, vomiting, and loss of appetite due to dampness or summer heat. Additionally, it is used for stomach flu and acute gastritis in combination with other herbs, including *Agastache rugosa*^{19,40}. *E. fortunei* contains alkaloids, which can be tumorigenic with excessive consumption⁴¹. Thus, it is important to check any decoction at regular doses for the absence of side effects. In this study, we demonstrated that oral administration of WEF at 50 mg/kg suppressed the pulmonary metastasis of B16F10 melanoma cells *in vivo* with no apparent adverse effects, suggesting that WEF can be used as a safe and effective remedy for cancer management.



In this study, we used CM from tumor cells as an inducer to stimulate endothelial cells for an *in vitro* angiogenesis assay to mimic *in vivo* tumor-induced angiogenesis. As reported by Ito *et al.*⁴², we observed that CM from HT1080 cells promoted the growth of HUVECs and increased tube formation on Matrigel. In contrast, WEF-treated tumor cells showed decreased production of MMP-9 in the CM; consequently, proteolytic activity against gelatin and collagen, and migration/invasion through Matrigel by WEF-treated cells were lower than those by control cells. WEF also inhibited the production of VEGF- α by tumor cells, thereby suppressing tumor-induced capillary-like tube formation and HUVEC migration. Furthermore, WEF-treated CM suppressed sprouting in an *ex vivo* aortic ring assay. In a Matrigel plug assay, the WEF-containing tumor xenograft showed not only a significant reduction in growth, but also decreased neovascularization, supporting the *in vivo* anti-angiogenic potency of WEF. WEF had no direct effect on endothelial cells in terms of migration, tube formation, or angiogenesis. Collectively, these results suggest that WEF has anti-metastatic and anti-angiogenic potency, targeting cancer cells but not endothelial cells.

In response to PMA stimulation, MAPK activation and subsequent NF- κ B activation occurred, resulting in MMP-9 activation, which is involved in cancer cell adhesion, invasion, and angiogenesis²⁶. In this study, we found that WEF almost completely blocked PMA-induced p38 and JNK phosphorylation, and dramatically decreased PMA-induced NF- κ B activation, consequently suppressing cellular metastatic potential by downregulating MMP-9 activity. PC-3 and HT1080 cells also produced high levels of VEGF under normoxic conditions, and WEF inhibited VEGF expression. Under hypoxic conditions, PC-3 and HT1080 cells accumulated HIF-1 α , which activates VEGF expression by binding the hypoxia response element in the VEGF promoter region, and which plays a pivotal role in tumor adaptation to the microenvironment. It has been reported that HIF-1 α is overexpressed in many human cancers and their metastatic foci, and it correlates with increased vessel density and resistance to chemo/radiotherapy³⁸. Thus, factors that regulate HIF-1 α activity are potential targets for cancer treatment. As shown in Figures 7C and S7, WEF inhibited hypoxia-induced HIF-1 α accumulation by suppressing Akt/mTOR signaling, supporting the finding that WEF inhibited PC-3 tumor xenograft growth and angiogenesis in nude mice (Figure 6C).

In summary, our data indicate that WEF exerted anti-metastatic and anti-angiogenic effects on malignant cancer cells both *in vitro* and *in vivo* by targeting key molecules involved in tumor progression, including MMP-9 and VEGF. Furthermore, we observed the potent therapeutic efficacy of WEF against pulmonary metastasis in mice, with no apparent side effects. These results indicate that WEF may be a candidate agent against malignant metastatic human cancers.

Methods

Cells. HT1080 cells (KCLB No. 10121, human fibrosarcoma), PC-3 cells (KCLB No. 21435, human prostate adenocarcinoma), and B16F10 cells (KCLB No. 80008, murine melanoma) were obtained from Korean Cell Line Bank (Seoul, Korea) in 2012, where they were characterized by DNA fingerprinting. Cells were maintained in RPMI1640 or Dulbecco's modified Eagle's medium (DMEM, Cellgro, Manassas, VA) supplemented with 10% (v/v) heat-inactivated fetal bovine serum (FBS; Cellgro) and 100 U/ml penicillin/100 μ g/ml streptomycin (Cellgro) at 37°C in a humidified 5% CO₂ incubator. Human umbilical vein endothelial cells (HUVECs) purchased from Innopharmascreen (Asan, Korea) in October 2012 were maintained in Endothelial cell Growth Medium-2 (EGM-2; PromoCell, Heidelberg, Germany) and used at passages 3 to 8. Cells were routinely screened for *Mycoplasma* contamination.

Animals. Specific pathogen-free (SPF) female C57BL/6J mice and athymic nude mice were purchased from Taconic Farms Inc. (Samtako Bio Korea, Osan, Korea) and Nara Biotech (Seoul, Korea), respectively. Male Sprague-Dawley rats were obtained from Taconic Farms Inc. (Samtako Bio Korea). Mice and rats were housed under constant conditions (12 h/12 h light/dark cycles at 22 \pm 1°C and 55 \pm 5% humidity) under SPF conditions. All animal experiments were performed according to the Guide for the Care and Use of Laboratory Animals of the National Institutes of Health

and approved by the Animal Care and Use Committee at Korea Institute of Oriental Medicine with a reference number of #13-67, #13-94, and #14-27.

Reagents and antibodies. Type A gelatin from porcine skin, type I collagen from calf skin, 3-(4,5-Dimethyl-2-thiazolyl)-2,5-diphenyltetrazolium bromide (MTT), phorbol 12-myristate 13-acetate (PMA), and mitomycin C were purchased from Sigma Chemical Co. (St. Louis, MO, USA). Growth factor-reduced Matrigel Basement Membrane Matrix was obtained from BD Biosciences (Bedford, MA, USA). Recombinant murine vascular endothelial growth factor 165 (rMu VEGF₁₆₅) and tumor necrosis factor- α (rMu TNF- α) were purchased from PromoKine (Heidelberg, Germany). Antibodies against MMP-9, I κ B α , pI κ B α , NF- κ B p65, p38, p-p38, ERK, p-ERK, JNK, p-JNK, Akt, p-Akt, mTOR, p-mTOR, TBP, and tubulin were obtained from Cell Signaling Technology (Danvers, MA, USA). Anti-HIF-1 α antibody was purchased from BD Bioscience (Pharmingen, San Diego, CA).

Preparation of WEF. Dried *E. fortunei* was purchased from Yeongcheon Oriental Herbal Market (Yeongcheon, Korea) and deposited in the herbal bank of KM-based Herbal Drug Development Group, Korea Institute of Oriental Medicine (KIOM; Daejeon, Korea) after verifying by Professor Ki Hwan Bae of the College of Pharmacy, Chungnam National University (Daejeon, Korea). Dried WEF (50 g) placed in 1 L D.W was heat-extracted at 115°C for 3 h in a Cosmos-600 Extractor (Gyeonseo Co., Incheon, Korea). The extract was filtered through a testing sieve (150 μ m, Retsch, Haan, Germany), evaporated on a rotary evaporator, and then concentrated by lyophilization. Freeze-dried WEF powder (50 mg) was dissolved in 1 ml 10% DMSO (v/v) and filtered through a 0.22 μ m disk filter.

Safety assessment after oral administration of WEF. C57BL/6J mice (n=3 per group) at 5 weeks of age were fed vehicle (saline) or 50 mg/kg WEF daily for 15-day experimental period. Body weight was daily measured and gross appearance and behavior were carefully monitored. At the time of sacrifice, weight of major organs including heart, liver, lung, spleen, and kidneys were measured. Hematological and serological parameters were measured using ADVIA 2120i hematology system (Siemens Healthcare Diagnostics, Tarrytown, NY) and XL 200 (Erba Diagnostics Mannheim, Germany), respectively.

Cell cytotoxicity assay. To determine cytotoxicity of WEF, 5 \times 10³ cells were plated in 96-well culture plates, treated with various concentrations of WEF (10 to 500 μ g/ml) for 48 h, and then MTT assay was performed as described previously⁴³.

Anchorage-independent cell growth in soft agar. Cells (5 \times 10⁴) suspended in 2 ml medium with specified concentrations of WEF, 0.3% agar, and 10% FBS were plated over the bottom agar pre-solidified with 3 ml medium containing 0.6% agar and 10% FBS. Colony formation was daily observed under a phase-contrast microscope and colonies were photographed.

Wound healing cell migration assay. Cells plated on a 60-mm culture dish with 90% confluence were pre-treated with mitomycin C (25 μ g/ml) for 30 min to inhibit proliferation, and then an injury line with a width of 2 mm was made by scraping across the cell monolayer with sterile scraper. After floating cell debris was removed by washing with PBS, cell migration in the presence of WEF was monitored under a phase-contrast microscope and photographed.

Transwell migration and invasion. The ability of cells to migrate and invade was measured using a Transwell chamber with polycarbonate membrane (10 mm diameter, 8 μ m pore size) as described previously^{22,23}. For HUVECs migration, EGM-2, bFGF (1 μ g/ml), VEGF- α (100 ng/ml), or CM from cancer cells were used as attractant. For the collection of CM, cells were treated with WEF for 24 h in complete media conditions, washed twice with 0.5% serum media, and then incubated for another 24 h in 0.5% serum media.

In vivo pulmonary metastasis assay. B16F10 cells (3 \times 10⁵ cells/200 μ l PBS) were injected *via* the tail veins of C57BL/6J mice. Mice were randomly divided into 2 groups (n=4 for each group) and started to administrate vehicle (saline) or 50 mg/kg WEF (day 0). After daily administration for 17 days, mice were sacrificed and lungs were fixed in Bouin's solution (Sigma) for counting black colonies macroscopically.

Reverse transcription and polymerase chain reaction (RT-PCR). Total RNA was extracted using RNA extraction solution (BioAssay Co., Daejeon, Korea) and 3 μ g RNA was reverse transcribed to cDNA using 1st Strand cDNA Synthesis kit (BioAssay Co.) according to the manufacturer's instruction. The cDNA aliquots were analyzed by semi-quantitative PCR. After PCR products were electrophoresed on agarose gels and stained with GreenLight™ (BioAssay Co., Daejeon, Korea), band intensity was quantitatively analyzed using ImageJ software (National Institute of Health, USA).

Western blot analysis. Whole cell lysates and nuclear/cytosolic extracts were obtained using M-PER Mammalian Protein Extraction Reagent and NE-PER nuclear and Cytosolic Extraction Reagent (Thermo Scientific, Rockford, IL), respectively. Aliquots of protein resolved by SDS-PAGE were immunoblotted with specific antibodies and detected as described previously^{22,23}.

Zymography. Cells pre-incubated with WEF in serum-free media for 12 h were stimulated with 5 nM PMA for an additional 24 h. Collected serum-free CM were



electrophoresed on an 8% SDS-PAGE containing 0.1% gelatin or 4 mg/ml collagen. After washing with washing buffer (50 mM Tris-HCl, pH7.5, 100 mM NaCl, 2.5% Triton X-100), gels were incubated in reaction buffer (50 mM Tris-HCl, pH7.5, 150 mM NaCl, 10 mM CaCl₂, 0.02% NaN₃, 1 μM ZnCl₂) at 37°C for 24 h. Gels were stained with Coomassie Brilliant Blue R-250 staining solution (Bio-Rad Laboratories, Hercules, CA, USA) and destained with 10% isopropanol/10% acetic acid (v/v) solution. Gelatinase and collagenase activities were visualized as clear bands against blue background.

Determination of VEGF level by ELISA. Cells were treated with indicated concentrations of WEF for 48 h and CM was collected by centrifugation at 12000 rpm for 10 min. The levels of VEGF in CM were determined with the Human ELISA Development kit (PeproTech, Rocky Hill, NJ, USA) according to the manufacturer's instruction.

Endothelial cell capillary-like tube formation assay. HUVEC tube formation assay was performed using an ECMatrix assay kit (Millipore, Temecula, CA, USA) according to the manufacturer's instruction. In brief, chilled ECMatrix (10 μl) was transferred to each well of a pre-cooled 1 μ-Slide Angiogenesis ibi-Treat chamber (ibidi GmbH, Germany) and allowed to solidify for 30 min at 37°C. HUVECs (5 × 10⁵ cells) suspended in WEF-treated CM (50 μl) were seeded onto the surface of polymerized ECMatrix and incubated for 8 h at 37°C in 5% CO₂. Tube networks were observed under phase-contrast inverted light microscopy and photographed. Tube formation was quantified by measuring area of these capillary-like structures in five fields of view in each well.

Matrigel plug assay. To evaluate tumor-induced angiogenesis, PC-3 cells (3 × 10⁶/100 μl serum-free medium) mixed in Matrigel (500 μl) with heparin (50 U/ml) and WEF were subcutaneously injected into the abdomen of athymic nude mice. At day 14 after implantation, Matrigel plugs were carefully removed and hemoglobin content in gel plugs was determined using a Drabkin's reagent kit (Sigma) as described previously³⁰. The concentration of hemoglobin was calculated based on the set of hemoglobin standard (Sigma).

Rat aortic ring sprouting assay. Dorsal aortas were isolated from 6-week-old Sprague-Dawley rats in a sterile manner and rinsed in cold PBS. Aortas were transversely cut into rings with 1 mm thickness using surgical blade, then each ring was placed in 48-well culture plates pre-coated with 100 μl of Matrigel and sealed with 40 μl of Matrigel. EGM-2 were added to the wells in a final volume of 400 μl and incubated for 3 days. After confirming sprouts emerged from the aortic rings and grew outward, medium was changed with control CM or WEF-treated CM and microvessel outgrowths were observed under phase-contrast inverted light microscopy and photographed.

Statistical analysis. The values were represented as means ± standard deviation (SD). Statistical significance of the difference between groups was analyzed by Two-way analysis of variance (ANOVA) and Student's t-test with the SigmaPlot 8.0 software. P value less than 0.05 was considered significantly different.

1. Kumar, S. & Weaver, V. M. Mechanics, malignancy, and metastasis: the force journey of a tumor cell. *Cancer Metastasis Rev* **28**, 113–127 (2009).
2. Patel, L. R., Camacho, D. F., Shiozawa, Y., Pienta, K. J. & Taichman, R. S. Mechanisms of cancer cell metastasis to the bone: a multistep process. *Future Oncol* **7**, 1285–1297 (2011).
3. Westermarck, J. & Kahari, V. M. Regulation of matrix metalloproteinase expression in tumor invasion. *FASEB J* **13**, 781–792 (1999).
4. Rundhaug, J. E. Matrix metalloproteinases, angiogenesis, and cancer: commentary re: A. C. Lockhart *et al.*, Reduction of wound angiogenesis in patients treated with BMS-275291, a broad spectrum matrix metalloproteinase inhibitor. *Clin Cancer Res* **9**, 551–554 (2003).
5. Deryugina, E. I. & Quigley, J. P. Matrix metalloproteinases and tumor metastasis. *Cancer Metastasis Rev* **25**, 9–34 (2006).
6. Mira, E. *et al.* Secreted MMP9 promotes angiogenesis more efficiently than constitutive active MMP9 bound to the tumor cell surface. *J Cell Sci* **117**, 1847–1857 (2004).
7. Zheng, H. *et al.* Expressions of MMP-2, MMP-9 and VEGF are closely linked to growth, invasion, metastasis and angiogenesis of gastric carcinoma. *Anticancer Res* **26**, 3579–3583 (2006).
8. Gondi, C. S. *et al.* Downregulation of uPA, uPAR and MMP-9 using small, interfering, hairpin RNA (siRNA) inhibits glioma cell invasion, angiogenesis and tumor growth. *Neuron Glia Biol* **1**, 165–176 (2004).
9. Folkman, J. Role of angiogenesis in tumor growth and metastasis. *Semin Oncol* **29**, 15–18 (2002).
10. Kerbel, R. & Folkman, J. Clinical translation of angiogenesis inhibitors. *Nat Rev Cancer* **2**, 727–739 (2002).
11. Izawa, J. I. & Dinney, C. P. The role of angiogenesis in prostate and other urologic cancers: a review. *CMAJ* **164**, 662–670 (2001).
12. Folkman, J. & Klagsbrun, M. Angiogenic factors. *Science* **235**, 442–447 (1987).
13. Bicknell, R. Vascular targeting and the inhibition of angiogenesis. *Ann Oncol* **5 Suppl 4**, 45–50 (1994).

14. Gupta, M. K. & Qin, R. Y. Mechanism and its regulation of tumor-induced angiogenesis. *World J Gastroenterol* **9**, 1144–1155 (2003).
15. Appelmann, I., Liersch, R., Kessler, T., Mesters, R. M. & Berdel, W. E. Angiogenesis inhibition in cancer therapy: platelet-derived growth factor (PDGF) and vascular endothelial growth factor (VEGF) and their receptors: biological functions and role in malignancy. *Recent Results Cancer Res* **180**, 51–81 (2010).
16. Hui, Y. F. & Ignoffo, R. J. Angiogenesis inhibitors. A promising role in cancer therapy. *Cancer Pract* **6**, 60–62 (1998).
17. Papetti, M. & Herman, I. M. Mechanisms of normal and tumor-derived angiogenesis. *Am J Physiol Cell Physiol* **282**, 947–970 (2002).
18. Ushiki, J. H. *et al.* Medicinal plants for suppressing soil-borne plant diseases. *Soil Sci Plant Nutri* **42**, 423–426 (1996).
19. Chen, Y. F. *et al.* Relationship between antioxidant and antiglycation ability of saponins, polyphenols, and polysaccharides in Chinese herbal medicines used to treat diabetes. *J Med Plants Res* **5**, 2322–2331 (2011).
20. Jiang, J. K. L. *et al.* Terpenoids from Eupatorium fortunei TURCZ. *Helvetica chimica acta* **89**, 558–566 (2006).
21. Kim, Y. N., Koo, K. H., Sung, J. Y., Yun, U. J. & Kim, H. Anoikis resistance: an essential prerequisite for tumor metastasis. *Int J Cell Biol* **2012**, Article ID 306879, 11 pages (2012).
22. Kim, A., Im, M., Yim, N. H., Jung, Y. P. & Ma, J. Y. Aqueous extract of Bambusa caulis in Taeniam inhibits PMA-induced tumor cell invasion and pulmonary metastasis: suppression of NF-kappaB activation through ROS signaling. *PLoS One* **8**, e78061 (2013).
23. Kim, A. *et al.* Suppression of the invasive potential of highly malignant tumor cells by KIOM-C, a novel herbal medicine, via inhibition of NF-kappaB activation and MMP-9 expression. *Oncol Rep* **31**, 287–297 (2014).
24. Roomi, M. W., Monterrey, J. C., Kalinovsky, T., Rath, M. & Niedzwiecki, A. Patterns of MMP-2 and MMP-9 expression in human cancer cell lines. *Oncol Rep* **21**, 1323–1333 (2009).
25. Choi, J. H. *et al.* Suppression of PMA-induced tumor cell invasion and metastasis by aqueous extract isolated from Prunella vulgaris via the inhibition of NF-kappaB-dependent MMP-9 expression. *Food Chem Toxicol* **48**, 564–571 (2010).
26. Hwang, Y. P. *et al.* Suppression of PMA-induced tumor cell invasion by dihydroartemisinin via inhibition of PKCalpha/Raf/MAPKs and NF-kappaB/AP-1-dependent mechanisms. *Biochem Pharmacol* **79**, 1714–1726 (2010).
27. Reddy, K. B., Nabha, S. M. & Atanaskova, N. Role of MAP kinase in tumor progression and invasion. *Cancer Metastasis Rev* **22**, 395–403 (2003).
28. Yeh, C. B. *et al.* Antimetastatic effects of norcantharidin on hepatocellular carcinoma by transcriptional inhibition of MMP-9 through modulation of NF-kB activity. *PLoS One* **7**, e31055 (2012).
29. Zhao, K. *et al.* Wogonin suppresses melanoma cell b16-f10 invasion and migration by inhibiting ras-mediated pathways. *PLoS One* **9**, e106458 (2014).
30. Kim, A. *et al.* Suppression of NF-kappaB activity by NDRG2 expression attenuates the invasive potential of highly malignant tumor cells. *Carcinogenesis* **30**, 927–936 (2009).
31. Risau, W. Mechanisms of angiogenesis. *Nature* **386**, 671–674 (1997).
32. Jang, Y. J., Kim, D. S. & Jeon, O. H. Saxatilin suppresses tumor-induced angiogenesis by regulating VEGF expression in NCI-H460 human lung cancer cells. *J Biochem Mol Biol* **40**, 439–443 (2007).
33. Ye, J. & Yuan, L. Inhibition of p38 MAPK reduces tumor conditioned medium-induced angiogenesis in co-cultured human umbilical vein endothelial cells and fibroblasts. *Biosci Biotechnol Biochem* **71**, 1162–1169 (2007).
34. Grant, D. S. *et al.* Decorin suppresses tumor cell-mediated angiogenesis. *Oncogene* **21**, 4765–4777 (2002).
35. Fang, J. *et al.* Apigenin inhibits tumor angiogenesis through decreasing HIF-1alpha and VEGF expression. *Carcinogenesis* **28**, 858–864 (2007).
36. Staton, C. A. *et al.* Current methods for assaying angiogenesis in vitro and in vivo. *Int J Exp Pathol* **85**, 233–248 (2004).
37. Goodwin, A. M. In vitro assays of angiogenesis for assessment of angiogenic and anti-angiogenic agents. *Microvasc Res* **74**, 172–183 (2007).
38. Hirota, K. & Semenza, G. L. Regulation of angiogenesis by hypoxia-inducible factor 1. *Crit Rev Oncol Hematol* **59**, 15–26 (2006).
39. Qin, L. X. & Tang, Z. Y. The prognostic molecular markers in hepatocellular carcinoma. *World J Gastroenterol* **8**, 385–392 (2002).
40. Gan, R. Y. *et al.* Screening of natural antioxidants from traditional Chinese medicinal plants associated with treatment of rheumatic disease. *Molecules* **15**, 5988–5997 (2010).
41. Fu, P. P. Y., Y. C., Xia, Q., Chou, M. C., Cui, Y. Y. & Lin, G. Pyrrolizidine alkaloids-tumorigenic compounds in Chinese herbal medicines and dietary supplements. *J Food Drug Anal* **10**, 198–211 (2002).
42. Ito, Y., Iwamoto, Y., Tanaka, K., Okuyama, K. & Sugioka, Y. A quantitative assay using basement membrane extracts to study tumor angiogenesis in vivo. *Int J Cancer* **67**, 148–152 (1996).
43. Kim, A., Im, M., Yim, N. H., Kim, T. & Ma, J. Y. A novel herbal medicine, KIOM-C, induces autophagic and apoptotic cell death mediated by activation of JNK and reactive oxygen species in HT1080 human fibrosarcoma cells. *PLoS One* **9**, e98703 (2014).

Acknowledgments

This work has been supported by the Grant K14050 awarded to Korea Institute of Oriental Medicine (KIOM) from Ministry of Science, ICT and Future Planning (MSIP), Republic of Korea.



Author contributions

A.K. and J.Y.M. conceived the research; A.K. and M.J.I. designed the project; A.K. and M.J.I. performed most of the experiments; N.H.Y. helped the animal experiments; A.K. wrote the manuscripts; all authors reviewed the manuscript.

Additional information

Supplementary information accompanies this paper at <http://www.nature.com/scientificreports>

Competing financial interests: The authors declare no competing financial interests.

How to cite this article: Kim, A., Im, M., Yim, N.-H. & Ma, J.Y. Reduction of metastatic and

angiogenic potency of malignant cancer by *Eupatorium fortunei* via suppression of MMP-9 activity and VEGF production. *Sci. Rep.* 4, 6994; DOI:10.1038/srep06994 (2014).



This work is licensed under a Creative Commons Attribution-NonCommercial-NoDerivs 4.0 International License. The images or other third party material in this article are included in the article's Creative Commons license, unless indicated otherwise in the credit line; if the material is not included under the Creative Commons license, users will need to obtain permission from the license holder in order to reproduce the material. To view a copy of this license, visit <http://creativecommons.org/licenses/by-nc-nd/4.0/>